Single-Walled Carbon Nanotubes Functionalized with High Bonding Density of Polymer Layers and Enhanced Mechanical Properties of Composites

Long Xie, Feng Xu, Feng Qiu, Hongbin Lu,* and Yuliang Yang*

The Key Laboratory of Molecular Engineering of Polymers (Ministry of Education), Department of Macromolecular Science, Fudan University, Shanghai 200433, China

ABSTRACT: Single-walled carbon nanotubes (SWNTs) with high covalent bonding density of polymer layers have been prepared by a "grafting to" approach, where the benzyl chloride groups of styrene copolymers ($M_n =$ 47 600) reacted with the alkyne groups on SWNTs under relatively mild conditions, resulting in a higher grafting efficiency, as high as 81 wt % of (TGA). Microscopic observations clearly displayed the uniform, thick polymer layers formed on the SWNT surface. The high density of covalent bonding between polymer and nanotubes was confirmed by Raman, ^{1}H NMR, and FTIR, which makes them well dissolved in organic solvents and homogeneously dispersed in polymer matrices. The in situ UV−vis observations during the dissolution indicated that for such a multifunctional system almost no cross-links occurred between SWNTs due to the physical absorption and steric hindrance of polymer chains during the functionalization of SWNTs. The functionalized SWNTs exhibited a pronounced effect on the mechanical properties of polystyrene composites. Only 0.06 wt % of SWNTs resulted in 82% and 78% of increases in tensile strength and elastic modulus of the composites, respectively, indicating an efficient interfacial stress transfer between SWNTs and polymer.

Introduction

Single-walled carbon nanotubes (SWNTs) are deemed to be an ideal candidate as advanced filler materials in high-performance nanocomposites.[1] After nearly a decade of effort, however, the potential of SWNTs has not been fully realized; typically the mechanical properties of polymer nanocomposites still fall short of their theoretically predicted values. To optimize the final properties of nanocomposites, considerable work is focused on the interfacial molecular engineering of SWNTs, aiming at improving their dispersion in various host materials and state of interaction with organic macromolecules.[2] To date, two classes of main routes have been well established including covalent sidewall grafting reactions[3] and noncovalent exohedral interactions.[4] It has been well recognized that the strong chemical bonding at SWNTs−polymer interfaces makes for efficient load transfer from polymer matrix to SWNTs.[1,2]

The chemical bondings govern the load transfer between SWNTs and matrix and thus determine the mechanical properties of nanocomposites to a large extent. For a given diameter of SWNTs, its interfacial stress τ_{int} can be written as[5]

$$\tau_{int} = \tau_0 + \mu_{eff}(\partial V/\partial r) \tag{1}$$

where τ_0 is the initial threshold or critical stress upon pulling out a single nanotube from a polymer matrix and $\partial V/\partial r$ is the strain rate (V is the velocity of a nanotube and r is the pull-out displacement along the nanotube direction). μ_{eff} is the effective viscosity for interfacial sliding, which is closely related to the strength of interfacial bonding and to some extent reflects the efficiency of load transfer. Recent molecular simulations and experimental observations have showed some support to the above interfacial viscosity−stress relationship, where the interfacial shear strength between SWNTs and amorphous/

crystalline polymers increased with increasing interfacial chemical cross-links.[6,7] In addition, enhanced interfacial bonding contributes to the improvement of the fracture behavior of nanocomposites. As the crack reaches the nanotube surface, more covalent bondings can effectively inhibit the propagation of the cracks along the nanotubes.[8] As a consequence, a rational interface design is becoming more and more important for taking full advantages of nanotubes in polymer materials.

Increasing the covalent bonding density and molecular weight of polymers grafted on the SWNT surface is desirable to optimize the mechanical properties of SWNT−polymer composites.[1,2] The chemical bonding will introduce defects and decrease the strength of SWNTs, e.g., theoretical calculations predicted ∼15% of decrease in the maximum buckling force of nanotubes due to covalent functionalizations;[9] however, the bulk mechanical performance of composites largely depends on the interfacial stress transfer efficiency rather than exclusively on the strength of SWNTs. Recently, Coleman et al. systematically studied the effect of the defects introduced by chemically bonding on the mechanical properties of carbon nanotube−polymer nanocomposites.[10] Significant increases in Young's modulus were observed in all the cases, whether or not the nanocomposites contain a large amount of defects. It has been attributed to the fact that the polymer−nanotube interfacial stress transfer is so low, typically less than 50 MPa,[11] that the full potential of nanotubes might never be achieved. In addition, Gao and Haddon et al. demonstrated that the Young's modulus and tensile strength of nylon-6 composites increased 80% and 43%, respectively, as the concentration of carboxylic acid groups on SWNT surface increased to 6.8% from 0.0%.[12] Apparently, it is still a critical issue for the current case how to achieve efficient interfacial stress transfer in developing high-performance polymer materials, which may play a key role in maximizing the mechanical properties of SWNT-based composites.

* Corresponding authors: Fax +86-21-6564-0293; Tel 86-21-55664589; e-mail hongbinl@fudan.edu.cn, yuliangyang@fudan.edu.cn.

For the covalent functionalization of SWNTs, two strategies have been well established, i.e., "grafting from" and "grafting to" approaches.[2,3] The former allows high bonding density, the amount of grafting polymers even as high as 70 wt %, but control over the molecular weight and architecture of grafting polymers might be difficult. In contrast, the latter is a modular approach in which polymers can be prepared prior to the grafting step, and thus their molecular size and architecture can be well controlled. Various polymers have been successfully grafted onto the nanotube surface via the "grafting to" strategy involving radical coupling,[13] nitrene addition,[14] click coupling,[3a] nucleophilic reaction of polymeric carbanions,[15] and reactions with carboxyl groups on oxidized SWNTs.[16] Typically, however, the grafting density of SWNTs via the "grafting to" approach is low due to the steric hindrance of polymer chains, and furthermore, the grafting reactions require harsh conditions, e.g., high temperature and long reaction times. In addition, the molecular weight of grafting polymers in the literature is often not high enough, e.g., $M_n < 20\,000$, which is favorable for the dispersion of SWNTs in polymers, but they are probably too short to form sufficient entanglements with the bulk polymer. In a recent work, polystyrene with $M_n \sim 30\,000$ has been grafted to multiwalled carbon nanotubes (MWNTs) by a TEMPO radical approach, but again, a low grafting density (only 24 wt %) was obtained.[17] Obviously, in the existing "grafting to" approach one has to balance the molecular weight and grafting density of polymers as considering the steric hindrance of polymer chains. It is highly desirable to develop a convenient route that can simultaneously increase the molecular size and bonding density of grafted polymers.

In this work, we report an efficient "grafting to" method to increase the covalent bonding density at SWNT−polymer interface in which the multifunctional block polymers with molecular weight close to 50 000 are grafted to the SWNT surface. By exploiting the reaction between benzyl chloride and alkyne,[18] the polymer grafting was completed under the mild condition, and the thick polymer layers attached on the SWNTs surfaces were obtained in a relatively short time. Such a grafting efficiency has never been achieved before, upon using other "grafting to" approaches. The high bonding density and molecular size of grafting polymers improved the stress transfer and chain entanglements and therefore pronouncedly reinforced the mechanical properties of the resulting composites even at relatively low SWNT concentrations.

Experimental Section

Materials. SWNTs were purchased from Shenzhen Nanotech Port Co. (China). Styrene (St, Yonghua Special Chemicals, 99%) and *p*-chloromethylstyrene (CMS, Aldrich, 97%) were freshly distilled over calcium hydride under reduced pressure and stored under nitrogen in a refrigerator prior to use. Tetrahydrofuran (THF, Shanghai Feida, 99.5%) was refluxed over sodium and distilled. 2,2′-Azobis(isobutyronitrile) (AIBN, Shanghai 4th Factory of Chemicals, 99%) was recrystallized from methanol. 2,2,6,6-Tetramethyl-1-piperidineoxy (TEMPO, Acros, 98%), sodium hydrogen carbonate (NaHCO$_3$, Shanghai Qingxihua, 99.5%), 1,2-dichlorobenzene (ODCB, Fluka, 99%), isoamyl nitrite (Fluka, 97%), triphenylphosphine (PPh$_3$, Fluka, 98.5%), bis(triphenylphosphine)-palladium(II) dichloride (PdCl$_2$(PPh$_3$)$_2$, Fluka, 98%), *p*-aminophenylalkyne (Aldrich, 97%), acetonitrile (Shanghai Lingfeng, 99.8%), toluene (Shanghai 1st Factory of Chemicals, 99%) and *N,N*′-dimethylformamide (DMF, Shanghai 1st Factory of Chemicals, 99%) were used as received. Polystyrene with molecular weight $M_n = 66\,961$ and $M_w/M_n = 3.4$ (Chimei Co., China) was used as the polymeric matrix for SWNT composites in this study.

Purification of SWNTs. 100 mg of SWNTs placed in a 250 mL flask was oxidized in wet air at 250 °C for 3.5 h, followed by continuous stirring for 24 h in concentrated hydrochloric acid at room temperature. After thorough washing with a large amount of deionized water, the obtained SWNTs were dried at 100 °C under vacuum overnight and then used for further functionalizations.

Preparation of APA-SWNT.[19] 8 mg of SWNTs was sonicated for 10 min in 10 mL of 1,2-dichlorobenzene (ODCB) in an ice/water bath. To this suspension was added a solution of the *p*-aminophenylalkyne (APA) (2.6 mmol, 4 equiv/mol of carbon) in 5 mL of acetonitrile. After transferring to a septum-capped reaction tube (Ace Glass, #8648-03) and bubbling with nitrogen for 10 min, 4.0 mmol of isoamyl nitrite was quickly added. The septum was removed and replaced with a Teflon screw cap, and the suspension was stirred for 15 h at 60 °C. (CAUTION! Considerable pressure will be obtained in the vessel due to the emission of nitrogen. This can be alleviated by partially unscrewing the cap (for venting) every 30 min in the first 3 h.) After cooling to 45 °C, the suspension was diluted with 30 mL of DMF and filtered over a 0.45 *μ*m PTFE microporous membrane. The obtained APA-SWNTs were washed thoroughly using DMF with the assistance of sonication and then dried under vacuum overnight.

Preparation of Copolymers of Styrene and *p*-Chloromethylstyrene (PS-*co*-PCMS).[20] In a typical St and CMS copolymerization, 110 mL (0.965 mol) of St and 15 mL (0.106 mmol) of CMS were placed in a glass flask containing 0.49 g (3.1 mmol) of TEMPO (unimolecular initiator). After three freeze−thaw cycles, the glass flask was sealed off from the vacuum line and placed in an oil bath at 125 °C for 12 h. The resulting copolymer was dissolved in toluene and precipitated in methanol twice. The polymer was thoroughly dried under vacuum, until constant weight.
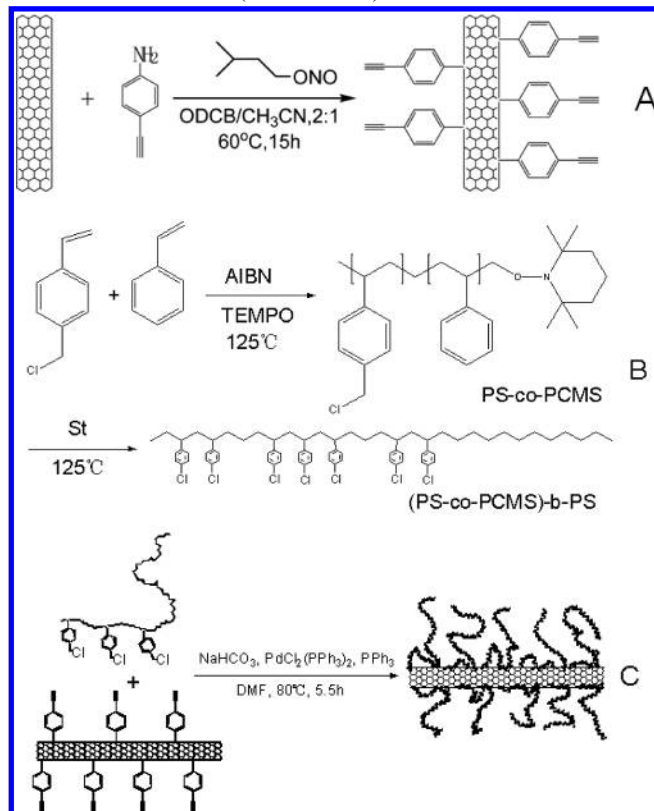
Preparation of (PS-*co*-PCMS)-*b*-PS. 20 g (1 mmol) of PS-*co*-PCMS (end-capped by TEMPO) was dissolved in 95 mL of St. After three freeze−thaw cycles, the mixture was sealed off from the vacuum line and was immersed in an oil bath at 125 °C for 5 h. The product was diluted in toluene, filtered, and fractionated with a toluene/methanol mixture to isolate the (PS-*co*-PCMS)-*b*-PS from the residual PS-*co*-PCMS. The obtained polymer was precipitated in methanol and dried under vacuum until constant weight.

Preparation of (PS-*co*-PCMS)-*b*-PS Functionalized SWNTs.[18] 3 mg of APA-SWNTs was dispersed in 15 mL of DMF by sonicating for 5 min at room temperature; (PS-*co*-PCMS)-*b*-PS (2 g, ∼2 mmol of benzyl chlorine groups), PPh$_3$ (2 mg, ∼0.007 mmol), PdCl$_2$(PPh$_3$)$_2$ (5 mg, ∼0.007 mmol), and NaHCO$_3$ (0.84 g, 10 mmol) were then added to the above dispersion and kept at 80 °C for 5.5 h with vigorous stirring. At the end of the reaction, the mixture was cooled to room temperature, diluted with 30 mL of DMF, and filtered with a 0.450 *μ*m PTFE microporous membrane. After thoroughly washing with DMF, the product was dried at 50 °C under vacuum overnight. The samples for HR-TEM observations were prepared by dispersing the functionalized SWNTs in DMF and depositing them onto copper grids. The samples for SEM observations were prepared from the THF solution by spin-casting on mica and drying at 50 °C under vacuum overnight.

Preparation of PS Films Containing SWNTs. All film samples were prepared by a solution spin-casting method. Different mass fractions of functionalized SWNTs were mixed with the PS/THF solution, and subsequently, sonication was imposed for 20 min to remove trapped air bubbles in solution and achieve the homogeneous nanotube dispersion. The SWNT composite films obtained by spin-casting on a Teflon-coated aluminum flake (100 mm diameter) were dried in vacuum for 72 h at 80 °C and overnight at 100 °C, before the mechanical tests and their thickness was controlled to be around 70 ± 5 *μ*m.

Characterizations. Gel permeation chromatography (GPC) was performed on a Agilent-1100 series GPC system equipped with a PL GEL linear column (5 *μ*m, pore size: 500 Å), two PL GEL mixed columns (molecular weight limits ranging from 200 to 3 × 10^6 g mol^{-1}), and a HP1100 RI detector HP1100 VWD detector, using THF as eluent at a flow rate of 1 mL/min at 35 °C. The system was calibrated by polystyrene standards (M_w range: 200−3 × 10^6 Da). The number-average molecular weight, M_n, and

Scheme 1. Illustrative Schemes for the Functionalization of SWNTs: (A) Functionalize SWNTs with APA; (B) Synthesis of (PS-*co*-PCMS)-*b*-PS; (C) Functionalize SWNTs with (PS-*co*-PCMS)-*b*-PS

Table 1. Molecular Characteristic of PS-*co*-PCMS and (PS-*co*-PCMS)-*b*-PS

PS-*co*-PCMS			(PS-*co*-PCMS)-*b*-PS	
$10^{-3}\bar{M}_n$	$\bar{M}_w/\bar{M}_n$	$N_{Cl}{}^a$	$10^{-3}\bar{M}_n$	$\bar{M}_w/\bar{M}_n$
20	1.20	21	47.6	1.25

[a] Calculated benzyl chlorine number in each chain of PS-*co*-PCMS according to NMR data.

bonded to the SWNTs surface via in situ generated diazonium species (Scheme 1A), which can further reacting with the benzyl chlorine groups appended on the polymer chains.[19] The diblock polymers containing benzyl chlorine, polystyrene-*co*-poly(*p*-chloromethylstyrene)-*b*-polystyrene ((PS-*co*-PCMS)-*b*-PS), were synthesized by the living free radical copolymerization of styrene and *p*-chloromethylstyrene and further polymerization with styrene as a second block.[20] Living free radical polymerization, which is a relatively active research field in recent years, allows one to conveniently construct a variety of macromolecules with complex architectures such as star, superbranched, and dendritic structures.[21] With TEMPO-based unimolecular initiators, we successfully introduced some benzyl chloride groups onto polystyrene chains to form the desired diblocks (Scheme 1B). The molecular parameters of the resulting block copolymers are given in Table 1. Their molecular weight distribution is narrow ($M_w/M_n = 1.20$ and 1.25, respectively), and the calculated benzyl chlorine number is 21 in each diblock copolymer chain.

As aforementioned, to optimize the mechanical properties of SWNT−polymer composites, it is desired to increase the covalent bonding density between SWNTs and polymer as well as the number of entanglement points at interface so that the interfacial stress transfer efficiency can be enhanced. For most of the reported "grafting to" approaches, however, their bonding density might be low due to the low reactive group number on polymer chains and the intrinsic steric hindrance effect. The entanglement between grafted polymer chains and bulk macromolecules is also not well established due to their molecular size of grafted polymers lower than the critical molecular weight to form physical entanglement. Typically, for example, the entanglement molecular weights for PS is 18 000,[22] which means that PS chains with $M_n > 20\,000$ should be used in order to better transfer stress to SWNTs. However, it has been demonstrated that increasing molecular weight would inevitably cause the decrease of grafting efficiency for end-functionalized polymers due to the entropy constraint of the polymer and the heterogeneous nature of the grafting reactions.[23] In this regard, increasing the reactive group number along high-M_n polymer chains is expected to be a possible approach in balancing the grafting density and physical entanglement at the interface of SWNT-based composites.

The coupling reaction between PS copolymer containing benzyl chloride and the alkyne groups on the SWNT surface is illustrated in Scheme 1C. It is for the first time, to the best of our knowledge, exploited to functionalize carbon nanotubes. The palladium (PdCl$_2$(PPh$_3$)$_2$)-catalyzed coupling reaction between benzyl chloride and alkyne was first used to synthesize propargylic compounds.[19] Its most attracting feature lies in the mild reaction condition and high reaction efficiency. The coupling reaction occurred in the present SWNT functionalization can be completed in less than 6 h, accompanying mechanically stirring at 80 °C. This is in contrast to the grafting reaction time even as high as several days reported in the literature.[13−16]

Figure 1 presents the Raman spectra of the purified SWNTs (Figure 1A), APA-SWNTs (Figure 1B), and (PS-*co*-PCMS)-*b*-

polydispersity index, M_w/M_n, were obtained using HP ChemStation for LC-3D (Rev. A. 06. 04) software. Thermogravimetric analysis (TGA) was performed on a NETZSCH TG209 instrument under a nitrogen atmosphere (20 mL/min), with a heating rate of 10 K/min from 100 to 700 °C. NMR was carried out on a Bruker (500 MHz) NMR instrument using CDCl$_3$ as solvent and tetramethylsilane as reference. Fourier transform infrared spectroscopy (FTIR) was performed on a Magna-550 instrument (potassium bromide pellet). Raman measurements were carried out on a Jobin Yvon LabRam-1B instrument using excitation laser with wavelength 632.8 nm. High-resolution transmission electron microscopy (HR-TEM) images for the fine nanostructures of purified and functionalized SWNTs were recorded on a JEOL JEM2010 electron microscope operating at 200 kV. Scanning electron microscopy (SEM, Philips XL30 FEG) was used to observe the microstructures of the SWNT/PS films and the nanostructures of purified and functionalized SWNTs. Filtration was completed using Teflon membranes (Millipore) of pore size around 450 nm. Mechanical testing was performed using an Instron mechanical testing system (model 5565 with Bluehill 2 software) with a 500 N load cell and pneumatic side-action grips. The tensile tests were carried out at 1 mm/min.

Results and Discussion

Synthesis and Characterizations of Functionalized SWNTs. SWNTs used in this work were produced by Shenzhen Nanotech Port Co. via the chemical vapor deposition method. The purification procedure removed most of the amorphous carbon and catalyst residuals on SWNTs, which can be confirmed by microscopic observations. To realize the covalently multibonding functionalization of nanotubes, alkynyl groups were first introduced onto the SWNT surface following a method developed by Jeffrey and co-workers[18] prior to the reaction with diblock polymers. With *p*-aminophenylalkyne as a generating reagent of the diazonium salt, a number of alkyne groups were
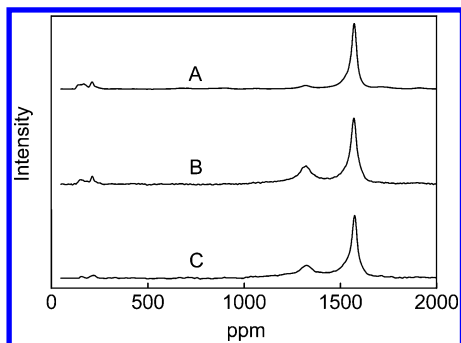
Figure 1. Raman spectra of three types of single-walled carbon nanotubes (SWNTs): (A) purified SWNTs, (B) APA-SWNTs, and (C) (PS-*co*-PCMS)-*b*-PS-SWNTs.
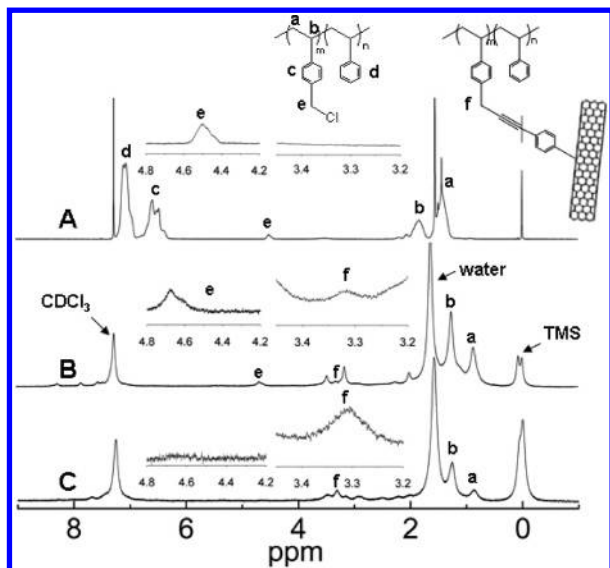

Figure 2. ^{1}H NMR (500 MHz, CDCl_3) spectra: (A) (PS-*co*-PCMS)-*b*-PS; (B) (PS-*co*-PCMS)-*b*-PS-SWNTs formed after the coupling reaction proceeds for 5.5 h; (C) (PS-*co*-PCMS)-*b*-PS-SWNT obtained after the coupling reaction proceeds for 48 h.
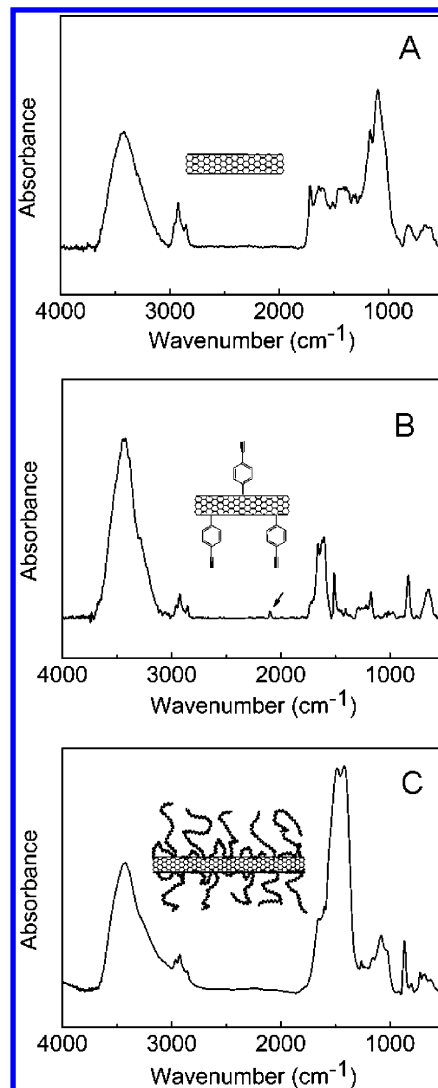

Figure 3. Fourier transform infrared (FTIR) spectra were performed on a Magna-550 instrument (KBr pellet): (A) purified SWNTs, (B) APA-SWNTs, and (C) (PS-*co*-PCMS)-*b*-PS-SWNTs.

PS-SWNTs (Figure 1C) using the excitation laser of wavelength 632.8 nm. Figure 1A exhibits the characteristic radial breathing $(50-170 \ cm^{-1})$ and tangential $(\sim 1570 \ cm^{-1})$ modes. A relatively weak disorder band $(\sim 1320 \ cm^{-1})$ indicates the presence of a small number of sp^3-hybridized carbons within the nanotube framework, as reported previously.[24] When the sidewall of SWNTs is covalently modified by APA, a difference in the relative intensity of disorder band with respect to tangential modes becomes prominent, indicating that a large number of sp^2-hybridized carbons have been converted to sp^3-hybridization. Upon further reacting with the benzyl chlorine groups from (PS-*co*-PCMS)-*b*-PS, the breathing mode and disorder bands in the spectrum become weakened with respect to tangential bands, probably because the polymer molecules attached to the sidewall hinder the radial breathing and disorder oscillation motion.

The ^{1}H NMR spectra of (PS-*co*-PCMS)-*b*-PS and (PS-*co*-PCMS)-*b*-PS-grafted SWNTs can confirm high density of covalent bonding between polymers and SWNTs. Figure 2A reveals several typical NMR peaks of the copolymer, which is consistent with those reported in the literature.[25] Of them, the intensity of benzylic proton peak (*e*) gradually decreases with decreasing number of benzyl chlorine groups during the reaction, accompanying a downfield shift from δ 4.5 in Figure 2A to δ 4.69 in Figure 2B. The appearance of a new proton peak (*f*, δ 3.3) indicates the formation of benzylalkyne groups (as shown

in Figure 2B,C). The extremely weak peak (*e*) and the relatively strong peak (*f*) presented in Figure 2C imply the formation of more covalent bonding between diblock copolymer and SWNTs, and furthermore, diamagnetic ring currents in SWNTs induce significant upfield shifts of the proton peaks in CH$_2$ (*a*) and CH (*b*) groups, that is, from δ 1.42 and δ 1.82 to δ 0.88 and δ 1.27, respectively. Similar phenomena were also observed before.[26] This also reflects the existence of more covalent bondings and essentially accords with the recent theoretical predictions.[27]

FTIR can provide further information about the structures appended to the surface of the SWNTs. The mid-IR spectra of three kinds of nanotubes are presented in Figure 3. Different from the purified SWNTs (Figure 3A), a small, but clearly discernible, signal at 2109 cm^{-1} appears in Figure 3B of APA-SWNTs and is attributed to the C$-$C stretching frequency of the appended terminal alkyne groups. After the alkyne groups reacting with the benzyl chlorine groups from (PS-*co*-PCMS)-*b*-PS, the FTIR spectrum of the product (Figure 3C) reveals the characteristic signals for the polymer, indicating that the polymer had been grafted to the SWNT surface.[3a] For (PS-*co*-PCMS)-*b*-PS-SWNTs, the signal at 2109 cm^{-1} becomes indiscernible in Figure 3C and may be attributed to the increasing symmetry of substitute groups in alkyens; that is, the hydrogen
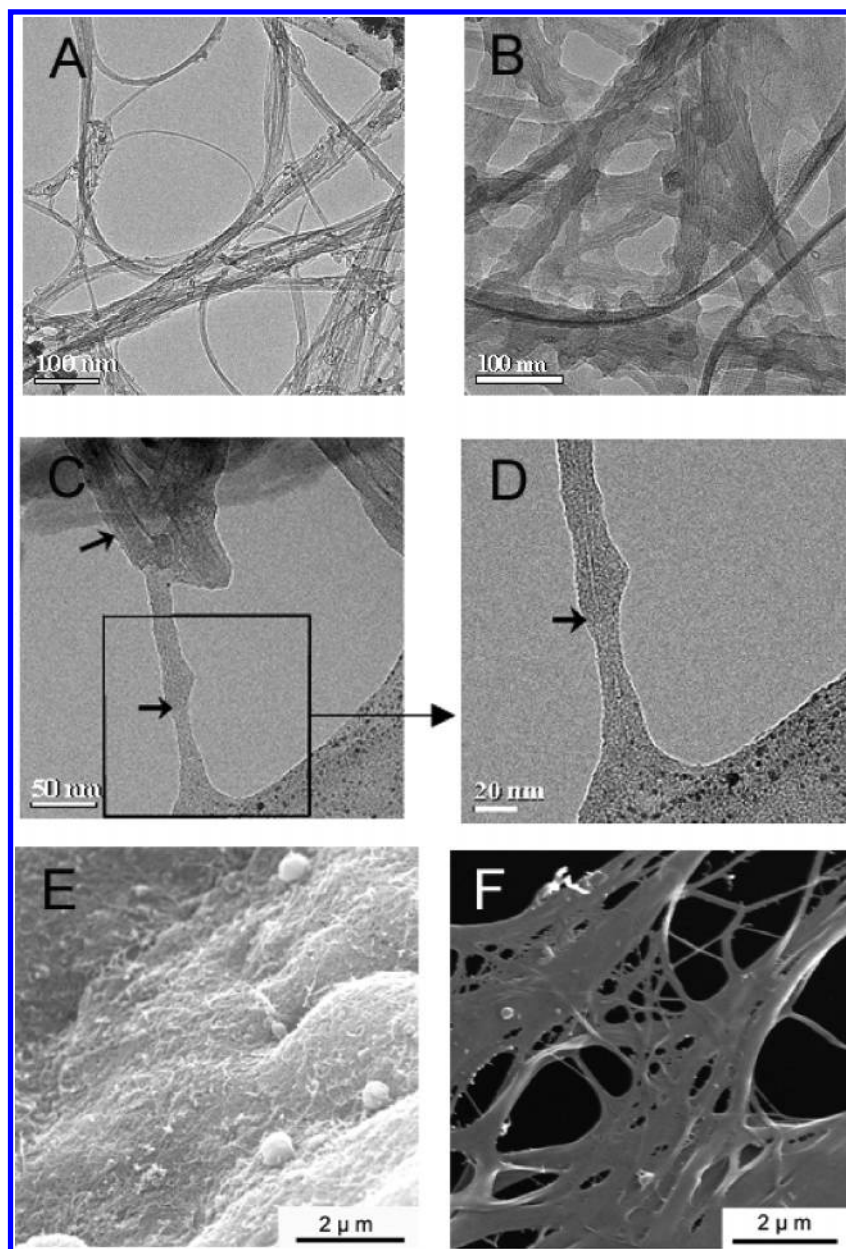
Figure 4. Electron microscopic images of two types of SWNTs. HR-TEM: (A) purified SWNTs, (B) (PS-*co*-PCMS)-*b*-PS-SWNTs, (C) an individual (PS-*co*-PCMS)-*b*-PS-SWNT, and (D) locally magnification of an individual (PS-*co*-PCMS)-*b*-PS-SWNT. SEM: (E) purified SWNTs and (F) (PS-*co*-PCMS)-*b*-PS-SWNTs.

in alkyne has been substituted by benzyl group from the diblock polymers.[28]

The fine nanostructures of purified and functionalized SWNTs were observed by high-resolution transmission electron microscopy (HR-TEM) and scanning electron microscopy (SEM). As shown in Figure 4A, the purification procedure used in our experiments removed most of the impurities residued in the pristine SWNTs, in spite of the presence of partial SWNTs in some aggregate form. After polymer functionalization, SWNTs became individualized and well coated with polymer (Figure 4B), which led to a remarkable increase in the diameter of SWNTs. The covalent wrapping of polymer to an individual nanotube can be clearly observed in Figure 4C,D, where an average polymer thickness of >6 nm is seen. In addition, SEM was used to observe the overall image of functionalized SWNTs, where the nanotubes were spin-casted on a freshly cleaved mica wafer from the THF solution. Figure 4E presents the morphology of the original nanotubes in which some curved nanotubes and aggregating particulates are visible. The morphology of

functionalized SWNTs is shown in Figure 4F. Similar to the case observed in the TEM images, a large amount of polymer was grafted on the nanotube surface. The aggregated morphology observed primarily originates from the poor affinity of mica to PS copolymer rather than the cross-linking between nanotubes (see below), which resulted in the agglomeration of polymer molecules during the evaporation of THF. These polymer-coated nanotube aggregates are readily dispersed in solvents under sonication. The dissolution experiments related to these functionalized SWNTs can be found in the next section.

The overall quantitative picture of the polymer layers grafted to the SWNTs surface can be obtained from TGA. As shown in Figure 5, the mass losses for (PS-*co*-PCMS)-*b*-PS-SWNTs (M_n = 47 600, M_w/M_n = 1.25 for diblock), PS-*co*-PCMS-SWNTs (M_n = 20 000, M_w/M_n = 1.20 for PS-*co*-PCMS), and the blank diblock polymers in nitrogen atmosphere mainly occurred at 260−440 °C with a maximum decomposition rate at ~400 °C. As further increasing temperature to 500 °C, the functionalized nanotubes remain stable whereas the blank
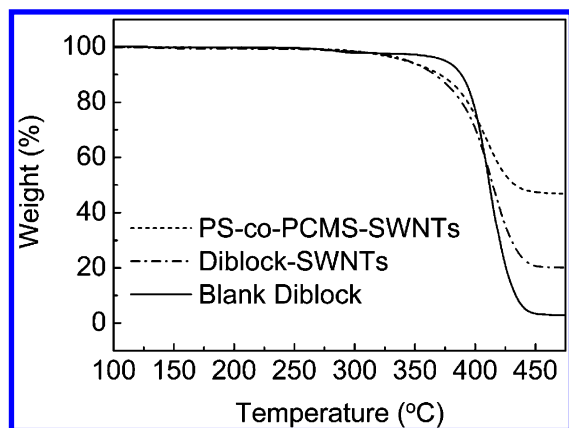
Figure 5. TGA curves of PS copolymer ((PS-*co*-PCMS)-*b*-PS) and SWNTs functionalized with PS-*co*-PCMS and diblock ((PS-*co*-PCMS)-*b*-PS); heating rate 10 °C/min and nitrogen atmosphere.

Figure 6. In situ UV−vis spectra during the dissolution of functionalized SWNTs in DMF. The time to record in the figure started after dissolving for 1 h, and these experiments were conducted on a Lambda 35 spectrophotometer using a quartz cuvette with 1 cm optical path length.

Figure 7. Photos for the dispersion status of SWNTs in different solvents: (A) purified SWNTs dispersed in THF; (B) (PS-*co*-PCMS)-*b*-PS-SWNTs in THF; (C) (PS-*co*-PCMS)-*b*-PS-SWNTs in toluene.

diblock polymer almost completely decomposes under the same conditions, except for a very small amount of residual carbon. The contents of the polymer layers calculated from the TGA data are 53% and 81% for PS-*co*-PCMS-SWNTs and (PS-*co*-PCMS)-*b*-PS-SWNTs, respectively. The slightly low starting decomposition temperature for grafting samples is similar to the reported phenomena and can be attributed to its increased thermal conductivity due to the addition of SWNTs.[29]

Such high grafting amounts is a striking result for the polymer-functionalized SWNTs by a "grafting to" approach. This primarily stems from the higher grafting density and the larger molecular size of polymers on SWNTs and is consistent qualitatively with the TEM observations. For the "grafting to" functionalization of nanotubes, it has been demonstrated that the increase in molecular weight of grafting polymers would decrease the grafting density of nanotubes. For example, the results reported by Chen and Yoon et al. showed that the amount of grafted poly(L-lactic acid) on MWNTs reduced to 25 wt % from 53 wt % as the molecular weight increased to 15 000 g/mol from 3000 g/mol.[30] The decreased grafting density was believed to be due to the increased steric hindrance for larger size polymer molecules. However, different from those end-functionalized polymers, such a steric hindrance effect can be partially compensated in the present multifunctional systems by increasing the number of functional groups on each polymer chain, and thus, the amount of grafted polymers depends on their molecular size to a large extent. In addition, the higher polymer grafting density relative to other "grafting to" approaches can reflect from the TEM images. For the end-functionalized poly-(L-lactic acid), the polymer only stained some parts of the MWNT surface with a squid-leg-like morphology as its molecular weight increases to >3000 g/mol.[30] In contrast, the present multifunctional system can create a more homogeneous grafting layer, as shown in Figure 4. Furthermore, the resulting morphology of functionalized nanotubes is more dependent on the site of alkyne groups or defects rather than on the molecular size of grafting polymers.

Solubility and Cross-Links of Polymer-Grafted SWNTs. The polymer-grafted SWNTs can be readily dissolved in organic solvents such as DMF, THF, and toluene using sonication (typically 5 min). When the sonication is stopped, a small amount of precipitate was formed slowly at the early stage of dissolution. After ∼1 h, the supernatants become to be homogeneous solutions. As shown in Figure 6, the in situ UV−vis spectra show only slight irregular fluctuation in absorbance intensity from 300 to 1100 nm, indicating the process of dissolving and precipitating of functionalized SWNTs ap-
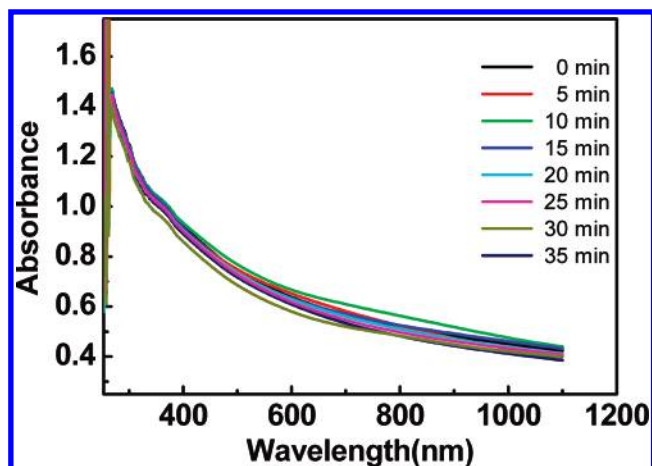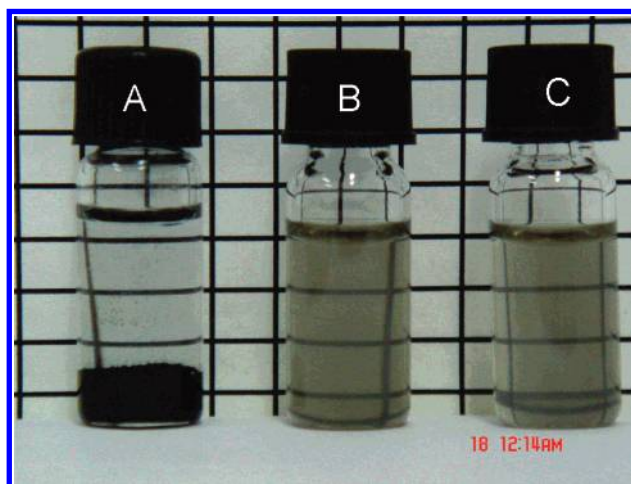
proaches the equilibrium. Figure 7 shows the dispersion status of pristine and grafted SWNTs in THF and toluene after removing the precipitates. The grafted SWNTs dissolved in THF and toluene result in clear, light-dark solutions while the purified SWNTs are almost insoluble in THF. The phenomena for diblock-grafted SWNTs are similar to those of (PCMS-*b*-PS)-grafted SWNTs. The molecular weight of the grafting polymers (diblock: $M_n = 47\ 600$; PCMS-*b*-PS: $M_n = 20\ 000$) seems not to exhibit a significant influence on the dissolution of grafted SWNTs in organic solvents. This is different from the experimental observations recently reported by Li and Adronov, where the molecular weight of grafting polymers displayed a significant impact on the solubility of SWNTs.[3a] The solubility dependence of SWNTs on molecular weight of the grafting polymers has been attributed to the decreased polymer grafting density and group reactivity at the chain ends as considering that a longer polymer chain tends to adopt a more random coil structure. However, for the present case higher grafting density exists at the polymer−SWNT interface due to more reactive groups on each polymer chain, despite its molecular weight much higher than those of grafting polymers reported in the reference. The insensitivity of solubility of grafted SWNTs on molecular weight of the grafting polymers is thus attributed to the improved grafting efficiency and thick interfacial polymer layers.

Scheme 2. Several Possible Grafting Regimes: i, Single Chain–Single Tube Bonding; ii, Single Chain–Multitube Bonding; iii, Physical Cross-Linking
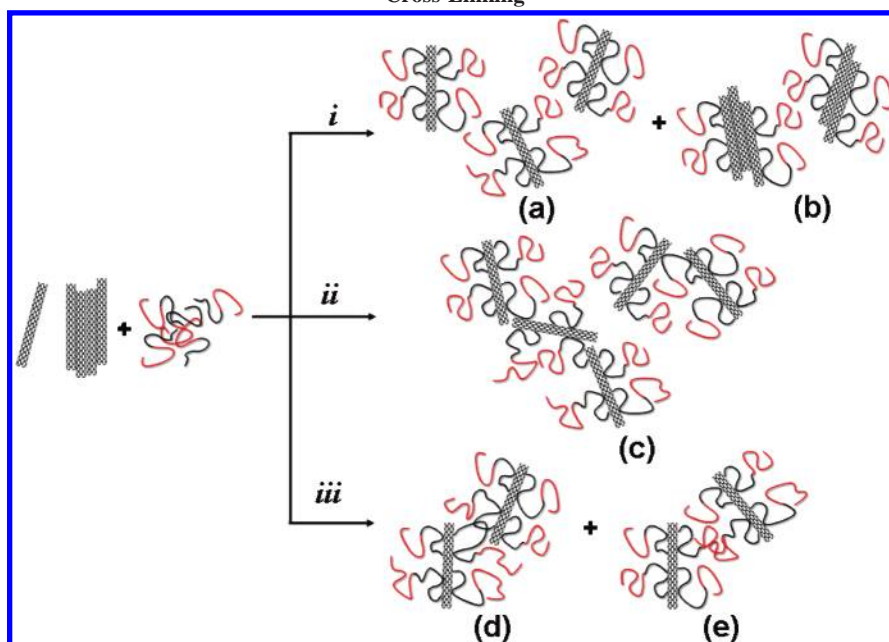
More reactive groups are able to enhance the grafting density of polymers but probably result in cross-linking between polymer chains and SWNTs and thus reduce the solubility of grafted SWNTs. This prompts us to analyze the origin of precipitate observed at the early stage of dissolution. For a system containing multifunctional polymer chains and SWNTs, there exist several possible grafting regimes, as illustrated in Scheme 2. For the regime i, single chain–single tube bonding, the reactive groups on a single chain prefer to react with the functional groups on the same nanotube, which results in polymer-coated exfoliated tubes (a) and tube bundles (b). However, after a benzyl chloride of a polymer chain reacts with an alkyne on a nanotube, the other benzyl chloride groups of the same polymer chain are still possible to react with the alkyne groups on other tubes: single chain–multitube bonding (regime ii). This results in the formation of cross-links between different tubes (chemical cross-linking). In addition, the polymer chains bonded onto the tubes probably form physical cross-links (regime iii) by chain entanglements (d and e) on account of the molecular weight of the grafting polymers (20 000 and 47 600) higher than the theoretical entanglement molecular weight (M_e ∼ 18 000 for PS). Among the above grafting modes, mode (a) is able to well dissolve in organic solvants and mode (e) is also able to dissolve but dependent on the conditions of solvent washing and sonication. Mode (b) can partially dissolve if the entanglement of carbon nanotube itself is not very serious, and in this case the use of sonication will be beneficial to the dissolution of less-entangled SWNTs. For mode (c), if the cross-linking density of tubes is salient, the precipitate will occur; otherwise, less cross-linked tubes are still or partially dissoluble, similar to the case that occurred in mode (b). The formation probability of grafting mode (d) should be relatively low in view of the distance between possible grafting points in the present cases. In reality, the origin of precipitate formation should primarily be from the regimes (b) and (c). Of them, the mode (b) should be the primary source instead of mode (c), in spite of involving less contribution from mode (c). In the following we present the possible explanations for this conjecture.

We first consider the possibility to form the intertube cross-links. To establish the covalent connection, the functional groups

of polymer chains and SWNTs need to approach each other. Once one covalent bond is created, the motion of the whole chain is subject to confinement of the tube and makes it preferentially absorbed on the tube surface in some profitable conformation. This immediately presents a steric hindrance for other chains and tubes and meanwhile imparts the other reactive groups on the same chain and the same tube more possibilities to complete covalent bonding. Recently, the physical absorption of common polymers on carbon nanotubes as a general phenomenon has been proposed.[31] For PS, the polymer adsorption which occurred concomitantly during the covalent functionalization of multiwalled carbon nanotubes has been reported, where about 5 wt % PS is still able to be absorbed on the tube surface, even after experiencing a thorough washing procedure.[31a] In addition, molecular dynamics simulation studies can provide a further support to the physical absorption of PS. Unlike the conjugated polymers containing aromatic rings on the backbone whose aromatic rings tend to align parallel to the tube surface, the plane of PS aromatic rings tends to be vertical to the surface of SWNTs.[32] This is also probably favorable to the reaction between the benzyl chloride of PS copolymers and the alkyne of SWNTs.

To further investigate the possible cross-linking occurred during the grafting reaction, the precipitate formed at the early stage of dissolution was collected and placed on the copper grids for TEM observations. The results show that the precipitate primarily involves the polymer–SWNT composite particulates with a size range of 2–5 μm (Figure 8). In these particulates slight intertube entanglement is discernible, but most of the SWNT bundles exhibited in purified SWNTs (Figure 4A) were exfoliated. Despite several times of solvent washing, there are some polymers molecules that remained within the interspace of tubes, which indicates the existence of the entanglement between polymer chains (regime iii). However, these chain entanglements are able to be untied as the particulates collected are redispersed in solvent with further sonication and a homogeneous solution is still achieved. Apparently, in the several possible grafting regimes aforementioned, the regime i is responsible for the functionalization in the present high bonding density approach and the well-exfoliated morphology
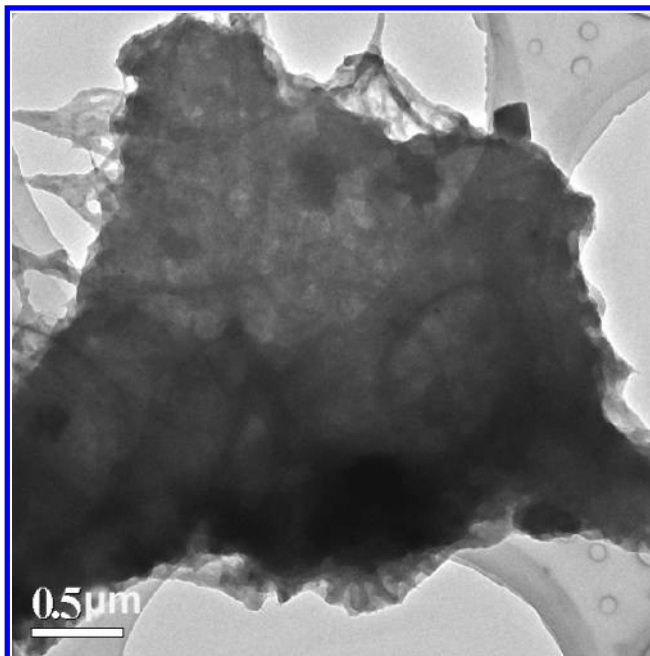
Figure 8. Representative TEM image of the precipitate formed at the early stage of dissolution in DMF.

Figure 9. Photos of PS composite films containing different SWNT contents, prepared by a solution spin-casting method. The tube content in composite films in the first row decreases from left to right (0.12, 0.06, 0.045 wt %), and the first one is the unfunctionalized SWNT−PS composite film (0.10 wt %); the tube content in the second row decreases from right to left (0.022, 0.015, 0.011 wt %), and the last one is the blank PS film.

can be achieved under sonication. The intertube cross-linking is negligible in view of the steric hindrance effect of grafted polymers.

Mechanical Properties of SWNT−PS Films. To examine the effect of the covalent bonding density between SWNTs and polymer on the mechanical properties of polymers, several polystyrene composite films containing different functionalized SWNT contents were prepared by a solution spin-casting method. The color of the resulting composite films gradually becomes light grayish from black with decreasing SWNT contents, as shown in Figure 9. The homogeneous dispersion of nanotubes in PS for different concentrations of composites indicates that the intertube cross-links are extremely few (if exists) and does not affect remarkably their exfoliation and distribution in polymer. This further supports the conjecture we proposed previously. For polymer nanocomposites the good dispersion of nanoparticles in matrix is a prerequisite to achieve
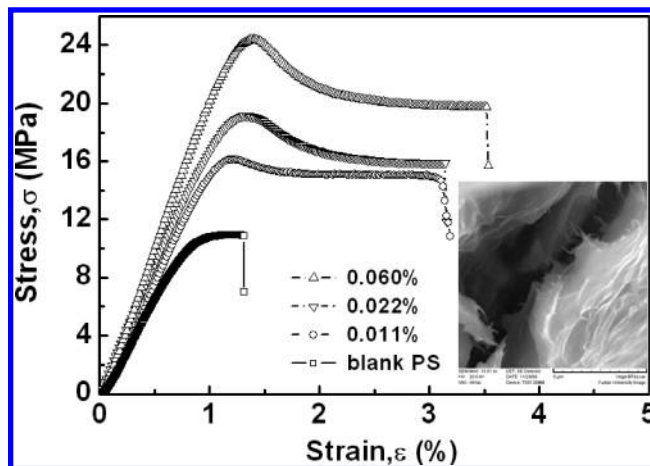

Figure 10. Stress−strain curves for PS composite films with the thickness of 70 ± 5 μm. The inset is the SEM image of the fractured surface of composite films containing 0.06 wt %, and the scale is 5 μm.

significant mechanical reinforcement. Even though there is no covalent bonding between nanoparticles and matrix, good particle dispersion in polymer can exhibit reinforcement effect to a certain extent. This has been reported for a variety of surfactant-assisted nanoparticle-filled polymers.[33] However, to further optimize the mechanical properties of materials, introducing more covalent linking points at interface is indispensable.

Representative tensile stress−strain curves for PS composites with different SWNT contents are shown in Figure 10. The blank PS film is brittle and usually displays relatively little plastic deformation. It exhibits ∼11 MPa in tensile strength, 1.5 GPa in tensile modulus, 1.5% in strain to failure, and no yield before failure, which is consistent with the results reported in the literature. The addition of SWNTs makes the composite films reveal obvious yield behavior prior to failure, and the stress-to-break for composite films steadily increases with increasing SWNT contents, from 10.8 MPa for neat PS to 19.7 MPa for the composite film containing 0.06 wt % SWNTs. The improvements in tensile strength σ_s and elastic modulus E_Y of these films are also clearly visible; the former is defined as the stress required to break the film, and the latter is defined as the slope of the stress−strain curve in the low strain linear region. As the SWNT content in PS increases to 0.06 wt %, the composite shows that σ_s and E_Y increase by 19.8 MPa and 2.6 GPa, respectively. This implies the increases of 82% in σ_s and 78% in E_Y relative to the blank PS. In addition, the effect of SWNTs on the toughness of PS is evident, and the latter is defined as the energy required to break the sample and can be obtained from the area under the stress−strain curve. Despite some irregularity in toughness of the films in our experiments, a remarkably increasing trend with SWNT content can be observed.

It is quite attractive that such low nanotube contents, 0.01−0.06 wt %, are able to significantly improve the modulus, strength, and toughness of PS. The pronounced reinforcement of extremely low amount of nanotubes in some polymer systems has been reported. In a recent investigation, Blond and Coleman et al. observed the simultaneous increases in strength and toughness of PMMA upon adding less than 0.15 wt % nanotubes functionalized via in situ PMMA polymerization.[34] The resulting materials exhibited the increases of 94, 360, and 1282% in Young's modulus, ultimate tensile strength, and toughness, respectively, relative to pure PMMA. Nevertheless, it should be noted that the reinforcement effect of nanotubes is actually polymer dependent. The reinforcement of nanotubes to PS is

distinct from that of PMMA.[35] The early PS−nanotube composites prepared by solution mixing under high-energy sonication exhibited increases of 36−42% and ∼25% in tensile modulus and strength upon adding 1 wt % of nanotubes.[35a] Recently, to improve the interfacial interaction between nanotubes and PS, the nanotubes were functionalized using chlorinated polypropylene (CPP) by an organometallic approach which resulted in further mechanical improvement: increases of 64% and 55% in modulus and toughness, respectively, upon the addition of 0.26 vol % nanotubes.[35c]

For the pronounced mechanical reinforcement observed in the present study, we attribute it to the good dispersion of SWNTs in PS and the outstanding interfacial stress transfer between SWNTs and polymers. Both of them originate from high polymer grafting density and covalent bonding density, which can be further confirmed by SEM observation of the materials. A typical morphology of the fracture surface of a composite film is presented as the inset of Figure 10, where some strip structures protruding from the matrix is clearly visible. Their size, much larger than that of diblock−SWNTs, expresses a high grafting efficiency and the good entanglement with bulk polymer. This is consistent with their excellent mechanical reinforcement. Consequently, the multifunctional polymer grafting method used herein allows one to construct a desired nanotube/polymer interface layer by means of a convenient "grafting to" approach. We believe it helpful for deepening the understating of physical or chemical issues in developing high-performance carbon nanotube-based composites.

Conclusions

We have developed a convenient approach that can effectively improve the bonding density at the interface of SWNTs and polymer by exploiting the coupling reaction between alkyne and benzyl chloride under relatively mild conditions. The high bonding density in functionalized SWNTs was confirmed by Raman, ^{1}H NMR, and FTIR spectroscopic results. Because of the physical absorption and steric hindrance of polymer chains, no or few cross-links between the SWNTs occurred during the functionalization of SWNTs even for such a multifunctional system. More functional groups on each polymer chain increase the reactive possibility between SWNTs and polymers and thus exhibited a higher polymer grafting efficiency in our experiments. TGA experiments revealed a weight loss of 81 wt % in nitrogen as the polystyrene copolymer of $M_n = 47\,600$ was grafted on the SWNT surface, which is in contrast to the results observed in other "grafting to" approaches. High interfacial bonding density and molecular weight of grafting polymers (more entanglement with bulk macromolecules) are able to effectively improve interfacial stress transfer and led to pronounced mechanical reinforcements of resulting composites.

The method proposed is especially useful for grafting high molecular weight polymers to SWNTs and could be helpful for resolving the problems met in other "grafting to" methods, for example, grafting density, entanglement between interfacial and bulk molecules, etc. In principle, the bonding density and the interfacial layer thickness can be tuned conveniently by altering the ratio of functional monomers to total monomers and the molecular weight of block polymers, respectively. This allows one to study systematically the effect of interfacial shear strength on macroscopic mechanical properties of SWNT-based composites and establish some fundamental understandings for further optimizing the final performance of SWNT−polymer composites.

Supporting Information Available: Experimental details. This material is available free of charge via the Internet at http://pubs.acs.org.

References and Notes

(1) (a) Coleman, J. N.; Khan, U.; Gun'ko Y. K. *Adv. Mater.* **2006**, *18*, 689. (b) Moniruzzaman, M.; Winey, K. I. *Macromolecules* **2006**, *39*, 5194.
(2) (a) Tasis, D.; Tagmatarchis, N.; Bianco, A.; Prato, M. *Chem. Rev.* **2006**, *106*, 1105. (b) Tjong, S. C. *Mater. Sci. Eng. R* **2006**, *53*, 73.
(3) (a) Li, H. M.; Cheng, F. Y.; Duft, A. M.; Adronov, A. *J. Am. Chem. Soc.* **2005**, *127*, 14518. (b) Kong, H.; Gao, C.; Yan, D. Y. *J. Am. Chem. Soc.* **2004**, *126*, 412.
(4) Chen, R. J.; Zhang, Y. G.; Wang, D. W.; Dai, H. J. *J. Am. Chem. Soc.* **2001**, *123*, 3838.
(5) Frankland, S. J. V.; Harik, V. M. *Surf. Sci.* **2003**, *525*, 103.
(6) (a) Qian, D.; Dickey, E. C.; Andrews, R.; Rantell, T. *Appl. Phys. Lett.* **2000**, *76*, 2868. (b) Frankland, S. J. V.; Caglar, A.; Brenner, D. W.; Griebel, M. *J. Phys. Chem. B* **2002**, *106*, 3046.
(7) Liao, K.; Li, S. *Appl. Phys. Lett.* **2001**, *79*, 4225.
(8) Desai, A. V.; Haque, M. A. *Thin-Walled Struct.* **2005**, *43*, 1787.
(9) Garg, A.; Sinnott, S. B. *Chem. Phys. Lett.* **1998**, *298*, 273.
(10) Cadek, M.; Coleman, J. N.; Ryan, K. P.; Nicolosi, V.; Bister, G.; Fonseca, A.; Nagy, J. B.; Szostak, K.; Beguin, F.; Blau, W. J. *Nano Lett.* **2004**, *4*, 353.
(11) Barber, A. H.; Cohen, S. R.; Wagner, H. D. *Appl. Phys. Lett.* **2003**, *82*, 4140.
(12) Gao, J. B.; Zhao, B.; Itkis, M. E.; Bekyarova, E.; Hu, H.; Kranak, V.; Yu, A. P.; Haddon, R. C. *J. Am. Chem. Soc.* **2006**, *128*, 7492.
(13) (a) Lou, X. D.; Detrembleur, C.; Sciannamea, V.; Pagnoulle, C.; Jerome, R. *Polymer* **2004**, *45*, 6097. (b) Liu, Y. Q.; Yao, Z. L.; Adronov, A. *Macromolecules* **2005**, *38*, 1172.
(14) Qin, S. H.; Qin, D. Q.; Ford, W. T.; Resasco, D. E.; Herrera, J. E. *Macromolecules* **2004**, *37*, 752.
(15) (a) Wu, W.; Zhang, S.; Li, Y.; Li, J. X.; Liu, L. Q.; Qin, Y. J.; Guo, Z. X.; Dai, L. M.; Ye, C.; Zhu, D. B. *Macromolecules* **2003**, *36*, 6286. (b) Blake, R.; Coleman, J. N.; Byrne, M. T.; McCarthy, J. E.; Perova, T. S.; Blau, W. J.; Fonseca, A.; Nagy, J. B.; Gun'ko, Y. K. *J. Mater. Chem.* **2006**, *16*, 4206.
(16) Lin, Y.; Zhou, B.; Fernando, K. A. S.; Liu, P.; Allard, L. F.; Sun, Y. P. *Macromolecules* **2003**, *36*, 7199.
(17) Lou, X. D.; Detrembleur, C.; Sciannamea, V.; Pagnoulle, C.; Jerome, R. *Polymer* **2004**, *45*, 6097.
(18) Laue, C. German Patent 4402915, 1995.
(19) Bahr, J. L.; Tour, J. M. *Chem. Mater.* **2001**, *13*, 3823.
(20) Tsoukatos, T.; Pispas, S.; Hadjichristidis, N. *Macromolecules* **2000**, *33*, 9504.
(21) (a) Hawker, C. J. *Acc. Chem. Res.* **1997**, *30*, 373. (b) Hadjichristidis, N.; Iatrou, H.; Pitsikalis, M.; Mays, J. *Prog. Polym. Sci.* **2006**, *31*, 1068.
(22) Fetters, L. J.; Lohse, D. J.; Milner, S. T.; Graessley, W. W. *Macromolecules* **1999**, *32*, 6847.
(23) (a) Baskaran, D.; Dunlap, J. R.; Mays, J. W.; Bratcher, M. S. *Macromol. Rapid Commun.* **2005**, *26*, 481. (b) Lou, X. D.; Detrembleur, C.; Sciannamea, V.; Pagnoulle, C.; Jerome, R. *Polymer* **2004**, *45*, 6097.
(24) (a) Bachilo, S. M.; Strano, M. S.; Kittrell, C.; Hauge, R. H.; Smalley, R. E.; Weisman, R. B. *Science* **2002**, *298*, 2361. (b) Strano, M. S.; Doorn, S. K.; Haroz, E. H.; Kittrell, C.; Hauge, R. H.; Smalley, R. E. *Nano Lett.* **2003**, *3*, 1091.
(25) Koloski, T. S.; Dulcey, C. S.; Haralson, Q. J.; Calvert, J. M. *Langmuir* **1994**, *10*, 3122.
(26) (a) Chen, J.; Liu, H. Y.; Weimer, W. A.; Halls, M. D.; Waldeck, D. H.; Walker, G. C. *J. Am. Chem. Soc.* **2002**, *124*, 9034. (b) Liu, A. H.; Honma, I.; Ichihara, M.; Zhou, H. S. *Nanotechnology* **2006**, *17*, 2845.
(27) Haddon, R. C. *Nature (London)* **1995**, *378*, 249.
(28) Socrates, G. *Infrared Characteristic Group Frequencies*; John Wiley & Sons: New York, 1980; pp 38−39.
(29) Liu, Y. Q.; Yao, Z. L.; Adronov, A. *Macromolecules* **2005**, *38*, 1172.
(30) Chen, G. X.; Kim, H. S.; Park, B. H.; Yoon, J. S. *J. Phys. Chem. B* **2005**, *109*, 22237.

(31) (a) Baskaran, D.; Mays, J. W.; Bratcher, M. S. *Chem. Mater.* **2005**, *17*, 3389. (b) Shvartzman-Cohen, R.; Levi-Kalisman, Y.; Nativ-Roth, E.; Yerushalmi-Rozen, R. *Langmuir* **2004**, *20*, 6085.

(32) Yang, M. J.; Koutsos, V.; Zaiser, M. *J. Phys. Chem. B* **2005**, *109*, 10009.

(33) (a) Gong, X. Y.; Liu, J.; Baskaran, S.; Voise, R. D.; Young, J. S. *Chem. Mater.* **2000**, *12*, 1049. (b) Shi, X. F.; Hudson, J. L.; Spicer, P. P.; Tour, J. M.; Krishnamoorti, R.; Mikos, A. G. *Nanotechnology* **2005**, *16*, S531.

(34) Blond, D.; Barron, V.; Kuether, M.; Ryan, K. P.; Nicolosi, V.; Blau, W. J.; Coleman, J. N. *Adv. Funct. Mater.* **2006**, *16*, 1608.

(35) (a) Qian, D.; Dickey, E. C. *Appl. Phys. Lett.* **2000**, *76*, 2868. (b) Coleman, J. N.; Blau, W. J.; Dalton, A. B.; Munoz, E.; Collins, S.; Kim, B. G.; Razal, J.; Selvidge, M.; Vieiro, G.; Baughman, R. H. *Appl. Phys. Lett.* **2003**, *82*, 1682. (c) Blake, R.; Coleman, J. N.; Byrne, M. T.; McCarthy, J. E.; Perova, T. S.; Blau, W. J.; Fonseca, A.; Nagy, J. B.; Gun'ko, Y. K. *J. Mater. Chem.* **2006**, *16*, 4206. (d) Chang, T. E.; Kisliuk, A.; Rhodes, S. M.; Brittain, W. J.; Sokolov, A. P. *Polymer* **2006**, *47*, 7740.